Relative Earthquake Hazard Maps
for selected urban areas in western Oregon

Canby-Barlow-Aurora

Lebanon

Silverton-Mount Angel

Stayton-Sublimity-Aumsville

Sweet Home

Woodburn-Hubbard

Molalla High School was condemned after the 1993 Scotts Mills earthquake (magnitude 5.6). A new high school was built on another site.

Oregon Department of Geology and Mineral Industries
Interpretive Map Series
IMS-8
Ian P. Madin and Zhenming Wang
1999

STATE OF OREGON
DEPARTMENT OF GEOLOGY AND MINERAL INDUSTRIES
Suite 965, 800 NE Oregon St., #28
Portland, Oregon 97232

Interpretive Map Series

IMS–8

Relative Earthquake Hazard Maps for Selected Urban Areas in Western Oregon

Canby-Barlow-Aurora, Lebanon, Silverton-Mount Angel,
Stayton-Sublimity-Aumsville, Sweet Home, Woodburn-Hubbard

By
Ian P. Madin and Zhenming Wang
Oregon Department of Geology and Mineral Industries

1999

Funded by the State of Oregon
and the U.S. Geological Survey (USGS), Department of the Interior,
under USGS award number 1434–97–GR–03118

CONTENTS

NOTICE

The results and conclusions of this report are necessarily based on limited geologic and geophysical data. The hazards and data are described in this report. At any given site in any map area, site-specific data could give results that differ from those shown on this map. **This report cannot replace site-specific investigations.** Some appropriate uses are discussed in the report. The hazards of an individual site should be assessed through geotechnical or engineering geology investigation by qualified practitioners.

IMS–8
Relative Earthquake Hazard Maps for Selected Urban Areas in Western Oregon

Canby-Barlow-Aurora, Lebanon, Silverton-Mount Angel, Stayton-Sublimity-Aumsville, Sweet Home, Woodburn-Hubbard

By Ian P. Madin and Zhenming Wang, Oregon Department of Geology and Mineral Industries

This is one of four companion publications presenting earthquake hazard maps for small to intermediate-sized communities in western Oregon. Each publication includes a geographic grouping of urban areas.

INTRODUCTION

Since the late 1980s, the understanding of earthquake hazards in the Pacific Northwest has significantly increased. It is now known that Oregon may experience damaging earthquakes much larger than any that have been recorded in the past (Atwater, 1987; Heaton and Hartzell, 1987; Weaver and Shedlock, 1989; Yelin and others, 1994). Planning the response to earthquake disasters and strengthening homes, buildings, and lifelines for power, water, communication, and transportation can greatly reduce the impact of an earthquake. These measures should be based on the best possible forecast of the amount and distribution of future earthquake damage. Earthquake hazard maps such as those in this publication provide a basis for such a forecast.

The amount of damage sustained by a building during a strong earthquake is difficult to predict and depends on the size, type, and location of the earthquake, the characteristics of the soils at the building site, and the characteristics of the building itself. At present, it is not possible to accurately forecast the location or size of future earthquakes. It is possible, however, to predict the behavior of the soil[1] at any particular site. In fact, in many major earthquakes around the world, a large amount of the damage has been due to the behavior of the soil.

The maps in this report identify those areas in selected Oregon communities that will be at higher risk, relative to other areas, during a damaging earthquake. The analysis is based on the behavior of the soils and does not depict the absolute earthquake hazard at any particular site. **It is quite possible that, for any given earthquake, damage in even the highest hazard areas will be light. On the other hand, during an earthquake that is stronger or much closer than our design parameters, even the lowest hazard categories could experience severe damage**.

This report includes a nontechnical description of how the maps were made and how they might be used. More technical information on the mapmaking methods is contained in the Appendix.

The printed report includes paper-copy *Relative Earthquake Hazard Maps* for each urban area, overlaid on U.S. Geological Survey topographic base maps at the scale of 1:24,000. In addition, for each area, three individual hazard component maps are included as digital data files on CD-ROM. The digital data are in two formats: (1) high-resolution -.JPG files (bitmap images) that can be viewed with many image viewers or word processors and (2) MapInfo® and ArcView® GIS vector files.

These maps were produced by the Oregon Department of Geology and Mineral Industries and were funded by the State of Oregon and the U.S. Geological Survey (USGS), Department of the Interior, under USGS award #1434-97-GR-03118. The views and conclusions contained in this document are those of the authors and should not be interpreted as necessarily representing the official policies, either expressed or implied, of the U.S. Government.

[1] In this report, "soil" means the relatively loose and soft geologic material that typically overlies solid bedrock in western Oregon.

EARTHQUAKE HAZARD

Earthquakes from three different sources threaten communities in western Oregon (Figure 1). These sources are crustal, intraplate, and subduction-zone earthquakes. The most common are crustal earthquakes, which typically occur in the North American plate above the subduction zone at relatively shallow depths of 6–12 mi (10–20 km) below the surface. The March 1993 earthquake at Scotts Mills (magnitude [M] 5.6) (Madin and others, 1993) and the September 1993 Klamath Falls main shocks (M 5.9 and M 6.0) (Wiley and others, 1993) were such crustal earthquakes.

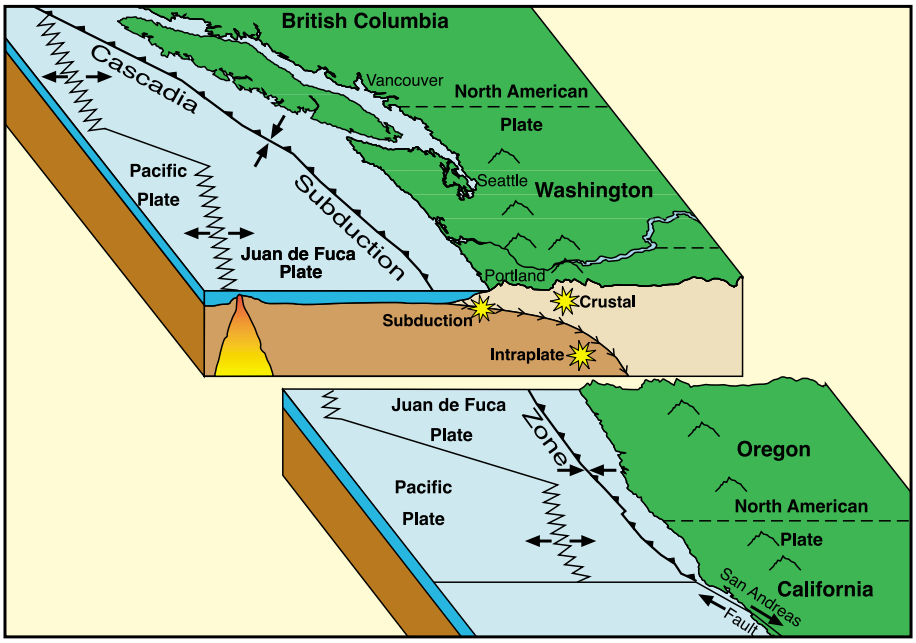

Figure 1. Plate-tectonic map of the Pacific Northwest. Oregon is cut in half to show where earthquakes originate below the surface (asterisks).

Deeper intraplate earthquakes occur within the remains of the ocean floor (the Juan de Fuca plate) that has been subducted beneath North America. Intraplate earthquakes caused damage in the Puget Sound region in 1949 and again in 1965. This type of earthquake could occur beneath much of western Oregon at depths of 25–37 mi (40–60 km).

Great subduction-zone earthquakes occur around the world where the plates that make up the surface of the Earth collide. When the plates collide, one plate slides (subducts) beneath the other, where it is reabsorbed into the mantle of the planet. The dipping interface between the two plates is the site of some of the most powerful earthquakes ever recorded, often having magnitudes of M 8 to M 9 on the moment magnitude scale. The 1960 Chilean (M 9.5) and the 1964 Great Alaska (M 9.2) earthquakes were subduction-zone earthquakes (Kanamori, 1977). The Cascadia subduction zone, which lies off the Oregon and Washington coasts, has been recognized for many years. No earthquakes have occurred on the Cascadia subduction zone during our short 200-year historical record. However, in the past several years, a variety of studies have found widespread evidence that very large earthquakes have occurred repeatedly in the past, most recently about 300 years ago, in January 1700 (Atwater, 1987; Yamaguchi and others, 1997). The best available evidence indicates that these earthquakes occur, on average, every 500 to 540 years, with an interval between individual events that ranges from 100–300 years to about 1,000 years (Atwater and Hemphill-Haley, 1997). We have every reason to believe that they will continue to occur in the future.

Together, these three types of earthquakes could cause strong shaking through most of western Oregon. Maps are available that forecast the likely strength of shaking for all of Oregon (Geomatrix Consultants, 1995; Frankel and others, 1996; Madin and Mabey, 1996). However, these maps show the expected strength of shaking at a firm site on bedrock and do not include the significant influence of soil on the strength of shaking. They forecast a uniform level of shaking and damage in most communities, and as such they do not provide a useful tool for planning earthquake hazard mitigation measures.

EARTHQUAKE EFFECTS

Damaging earthquakes will occur in the cities and towns of western Oregon. This fact was demonstrated by the Scotts Mills earthquake (M 5.6) in 1993 (Madin

and others, 1993). Although we cannot predict when the next damaging earthquake will strike, where it will occur, or how large it will be, we can evaluate the influence of site geology on potential earthquake damage. This evaluation can occur reliably even though the exact sources of earthquake shaking are uncertain.

The most severe damage done by an earthquake is commonly localized. One or more of the following phenomena generally will cause the damage in these areas:

1. Amplification of ground shaking by a "soft" soil column.

2. Liquefaction of water-saturated sand, silt, or gravel creating areas of "quicksand."

3. Landslides triggered by shaking, even on relatively gentle slopes.

These effects can be evaluated before the earthquake occurs, if data are available on the thickness and nature of the geologic materials and soils at the site (Bolt, 1993). Knowing the exact nature and magnitude of these effects is useful to technical professionals, and such data (in digital format) are included in this publication. For others, what is more significant is that these effects increase the damage caused by an earthquake and localize the most severe damage.

HAZARD MAP METHODOLOGY

Selection of map areas

Urban areas were mapped if they had a population greater than 4,000, were in Uniform Building Code (UBC) Seismic Zone 3 or 4, and were not likely to be the subject of a more detailed future hazard mapping program. The goal of this project was to provide an inexpensive general hazard assessment for small communities that could not afford their own mapping program but were not large enough to justify a major state-funded mapping effort. Such major, full-scale projects have been undertaken for the Portland, Salem, Eugene-Springfield, and Klamath Falls urban areas; they typically take several years and cost several hundred thousand dollars. In contrast, this project involved about two weeks of work and a few thousand dollars for each urban area mapped.

For each urban area selected, the hazard map area (inside the thick black line) was defined by the urban growth boundary plus a 3,300-ft (1-km)-wide buffer.

Geologic model

The most important element of any earthquake hazard evaluation is the development of a three-dimensional geologic model. For analysis of the amplification and liquefaction hazards, the most important feature is the thickness of the loose sand, silt, and gravel deposits that usually overlie firm bedrock. For an analysis of the landslide hazard, the steepness of the slopes and presence of existing landslides is important. For each urban area, the geologic model was developed as follows:

The best available geologic mapping was used to determine what geologic materials were present and where they occurred. Air photos were used to help make these decisions where the mapping was poor or of low resolution. All data were plotted digitally on USGS Digital Raster Graphics (DRG) maps (the digital equivalent of USGS 1:24,000-scale topographic maps).

Drillers' logs of water wells were examined to determine the geology beneath the surface and map the thickness of the loose surficial deposits and the depth to firm bedrock. Water wells were located according to the location information provided on the logs, which often is accurate only to within about 1,000 ft. Field location of the individual logs would have been prohibitively expensive.

The water well data were combined with the surface data to produce a three-dimensional geologic model, describing the thickness of the various geologic materials in the top 100 ft (30 m) throughout each urban area. For this procedure, MapInfo® and Vertical Mapper® Geographic Information System (GIS) software programs were used. The models take the form of a grid of thickness values spaced every 165 ft (50 m).

The resultant models were reviewed by geologists knowledgeable about each area, who judged whether the models were reasonable and consistent with the data.

Existing landslides were mapped where depicted on existing geologic maps or where air photos showed clear signs of landslide topography.

Slope data were derived from USGS Digital Elevations Models (DEMs) with elevation data every 100 ft (30 m). They were then used in MapInfo® and Vertical Mapper® to map the steepness of slopes.

The details of the local geology and data sources for each urban area are described in the "Urban Area Summaries" section of this report.

Table 1. *UBC-97 soil profile types. From ICBO, 1997*

Soil category	Description	Average shear-wave velocity meters/second	Amplification factor (Cv)
S_A	Hard rock	Vs > 1,500	0.8
S_B	Rock	760 < Vs < 1,500	1
S_C	Very dense soil and soft rock	360 < Vs < 760	1.5
S_D	Stiff soil	180 < Vs < 360	1.8
S_E	Soil	Vs < 180	2.8
S_F	Soil requiring site-specific evaluation		

Hazard analysis

Ground shaking amplification

The soils and soft sedimentary rocks near the surface can modify bedrock ground shaking caused by an earthquake. This modification can increase (or decrease) the strength of shaking or change the frequency of the shaking. The nature of the modifications is determined by the thickness of the geologic materials and their physical properties, such as stiffness.

This amplification study used a method first developed for the National Earthquake Hazard Reduction Program (NEHRP) and published by the Federal Emergency Management Agency (FEMA, 1995). This method was adopted in the 1997 version of the Uniform Building Code (ICBO [International Conference of Building Officials], 1997) and will henceforth be referred to as the UBC-97 methodology. The UBC-97 methodology defines six soil categories that are based on average shear-wave velocity in the upper 100 ft (30 m) of the soil column. The shear-wave velocity is the speed with which a particular type of ground vibration travels through a material, and can be measured directly by several techniques. The six soil categories are Hard Rock (A), Rock (B), Very Dense Soil and Soft Rock (C), Stiff Soil (D), Soft Soil (E), and Special Soils (F). Category F soils are very soft soils requiring site-specific evaluation and are not mapped in this study, because limited funding precluded any site visits.

For the amplification hazard component maps, we collected shear-wave velocity data (see Appendix for data and methods) at one or more sites in each urban area and used our geologic model to calculate the average shear-wave velocity of each 165-ft (50-m) grid cell in the model. We then assigned a soil category, using the relationships in Table 1.

According to the UBC-97 methodology, none of the urban areas in this study had Type A soils. UBC-97 soil category maps for each urban area are presented in the accompanying digital map set.

Liquefaction

Liquefaction is a phenomenon in which shaking of a saturated soil causes its material properties to change so that it behaves as a liquid. In qualitative terms, the cause of liquefaction was described very well by Seed and Idriss (1982): "If a saturated sand is subjected to ground vibrations, it tends to compact and decrease in volume; if drainage is unable to occur, the tendency to decrease in volume results in an increase in pore water pressure, and if the pore water pressure builds up to the point at which it is equal to the overburden pressure, the effective stress becomes zero, the sand loses its strength completely, and it develops a liquefied state."

Soils that liquefy tend to be young, loose, granular soils that are saturated with water (National Research Council, 1985). Unsaturated soils will not liquefy, but they may settle. If an earthquake induces liquefaction, several things can happen: The liquefied layer and everything lying on top of it may move downslope. Alternatively, it may oscillate with displacements large enough to rupture pipelines, move bridge abutments, or rupture building foundations. Light objects, such as underground storage tanks, can float toward the surface, and heavy objects, such as buildings, can sink. Typical displacements can range from centimeters to meters. Thus, if the soil at a site liquefies, the damage resulting from an earthquake can be dramatically increased over what shaking alone might have caused.

The liquefaction hazard analysis is based on the age and grain size of the geologic unit, the thickness of the unit, and the shear-wave velocity. Use of the shear-wave velocity to characterize the liquefaction potential follows Andrus and Stokoe (1997). Liquefaction

Table 2. *Liquefaction hazard categories*

Shear-wave velocity (meters/second)	Geologic units (see Appendix)			
	Qs, Qe, Qaf	Qmf, Qmf1, Qmf2, QPe, Qmt	Qac,QTac, QTaf, Qmc	Tbs, Tbv, Grus KJg, KJm
Greater than 200	Moderate	Low	None	None
100 to 200	High	Moderate	Low	None
Less than 100	High	High	Moderate	None

Thickness adjustment	
Unit thickness (m)	**Adjustment**
Less than 0.5	Down 2 categories
0.5 to 3.0	Down 1 category
Greater than 3.0	No change

hazard categories were assigned according to Table 2. In all communities we assumed that the susceptible units were saturated. This is reasonable and conservative, since most of the susceptible units are either alluvial deposits in floodplains, coastal deposits, or silt deposits in areas of low relief and high rainfall in the Willamette Valley.

Earthquake-induced landslides

The hazard due to earthquake-induced landsliding was assessed with slope data derived from USGS DEMs with 100-ft (30-m) data spacing and from mapping of existing slides, either from air photo interpretation or published geologic maps. The analysis was based on methods used by Wang, Y., and others (1998) and Wang, Z., and others (1999) but was greatly simplified because no field data were available. Earthquake-induced landslide hazard categories were assigned according to Table 3.

Table 3. *Earthquake-induced landslide hazard zones*

Slope angle (degrees)	Hazard category
Less than 5	Low
5 to 25	Moderate
Greater than 25	High
Existing landslides	High

RELATIVE EARTHQUAKE HAZARD MAPS

The *Relative Earthquake Hazard Map* is a composite hazard map depicting the relative hazard at any site due to the combination of the effects mentioned above. It delineates those areas that are most likely to experience the most severe effects during a damaging earthquake. Areas of highest risk are those with high ground amplification, high likelihood of liquefaction, existing landslides, or slopes steeper than 25°. Planners, lenders, insurers, and emergency responders can use these simple composite hazard maps for general hazard mitigation or response planning.

It is very important to note that the relative hazard map predicts the tendency of a site to have greater or lesser damage than other sites in the area. These zones, however, should not be used as the sole basis for any type of restrictive or exclusionary development policy.

The *Relative Earthquake Hazard Maps* were created to show which areas will have the greatest tendency to experience damage due to any combination of the three hazards described above. For the purpose of creating the final relative hazard map for each urban area, the zones in each of the three component maps were assigned numerical values according to Table 4.

For every point (in a 165-ft [30-m] grid spacing) on the map, the zone rating for each individual hazard type was squared, and the resulting numbers were added together. Then the square root of this sum was taken and rounded to the nearest whole number. A result of 4 or more was assigned to Zone A, 3 to Zone B, 2 to Zone C, and 1 to Zone D.

While the production of the individual hazard maps is different from previous DOGAMI relative earthquake studies (Wang and Priest, 1995; Wang and Leonard, 1996; Mabey and others, 1997), the method of production of the final relative hazard map is very similar. Thus, these relative hazard maps are directly comparable to DOGAMI studies in Eugene-Springfield, Portland, Salem, and Siletz Bay.

Table 4. *Hazard zone values assigned to the individual relative earthquake hazard map zones*

Relative hazard zone value	Amplification hazard (UBC-97 category S-)	Liquefaction hazard	Landslide hazard
0	B	None	None
1	C	Low	—
1.5	—	—	Moderate
2	D	Moderate	—
3	E	High	High

The GIS techniques used to develop these maps involved several changes between vector data and raster data, with a data grid cell size of 165 ft (50 m) for the raster data. As a result, the relative hazard maps often had numerous zones that were very small, and probably not significant. The final maps were hand-edited to remove all hazard zones that covered less than 1 acre.

USE OF RELATIVE EARTHQUAKE HAZARD MAPS

The *Relative Earthquake Hazard Maps* delineate those areas most likely to experience damage in a given earthquake. This information can be used to develop a variety of hazard mitigation strategies. The information should, however, be carefully considered and understood, so that inappropriate use can be avoided.

Emergency response and hazard mitigation

One of the key uses of these maps is to develop emergency response plans. The areas indicated as having a higher hazard would be the areas where the greatest and most abundant damage will tend to occur. Planning for disaster response will be enhanced by the use of these maps to identify which resources and transportation routes are likely to be damaged.

Land use planning and seismic retrofit

Efforts and funds for both urban renewal and strengthening or replacing older and weaker buildings can be focused on the areas where the effects of earthquakes will be the greatest. The location of future urban expansion or intensified development should also consider earthquake hazards.

Requirements placed on development could be based on the hazard zone in which the development is located. For example, the type of site-specific earthquake hazard investigation that is required could be based on the hazard.

Lifelines

Lifelines include road and access systems including railroads, airports, and runways, bridges, and over- and underpasses, as well as utilities and distribution systems. The Relative Earthquake Hazard Map and its component single-hazard maps are especially useful for expected-damage estimation and mitigation for lifelines. Lifelines are usually distributed widely and often require regional as opposed to site-specific hazard assessments. The hazard maps presented here allow quantitative estimates of the hazard throughout a lifeline system. This information can be used for assessing vulnerability as well as deciding on priorities and approaches for mitigation.

Engineering

The hazard zones shown on the *Relative Earthquake Hazard Maps* cannot serve as a substitute for site-specific evaluations based on subsurface information gathered at a site. The calculated values of the individual component maps used to make the Relative Hazard Maps may, however, be used to good purpose in the absence of such site-specific information, for instance, at the feasibility-study or preliminary-design stage. In most cases, the quantitative values calculated for these maps would be superior to a qualitative estimate based solely on lithology or non-site-specific information. Any significant deviation of observed site geology from the geologic model used in the analyses indicates the need for additional analyses at the site.

Relative hazard

It is important to recognize the limitations of a Relative Earthquake Hazard Map, which in no way includes information with regard to the probability of damage to occur. Rather, it shows that when shaking occurs, the damage is more likely to occur, or be more severe, in the higher hazard areas. The exact probability of such shaking to occur is yet to be determined.

Neither should the higher hazard areas be viewed as unsafe. Except for landslides, the earthquake effects that are factored into the Relative Earthquake Hazard Map are not life threatening in and of themselves. What is life threatening is the way that structures such as buildings and bridges respond to these effects.

The map depicts trends and tendencies. In all cases, the actual threat at a given location can be assessed only by some degree of site-specific assessment. This is similar to being able to say demographically that a zip code zone contains an economic middle class, but within that zone there easily could be individuals or neighborhoods significantly richer or poorer.

Because the maps exist as “layers” of digital GIS data, they can easily be combined with earthquake source information to produce earthquake damage scenarios. They can also be combined with probabilistic or scenario bedrock ground shaking maps to provide an assessment of the absolute level of hazard and an estimate of how often that level will occur. Finally, the maps can also be easily used in conjunction with GIS data for land use or emergency management planning.

This study does not address the hazard of tsunamis that exists in areas close to the Oregon coast and is also earthquake induced. The Oregon Department of Geology and Mineral Industries has published separate tsunami hazard maps on this subject (Priest, 1995; Priest and Baptista, 1995).

URBAN AREA SUMMARIES

CANBY-BARLOW-AURORA URBAN AREA

The Canby-Barlow-Aurora geologic model was developed using surface geologic data from Gannett and Caldwell (1998) and O'Connor and others (in press), examination of air photos, and subsurface data from 112 approximately located water-wells.

The geology of the area is relatively complex with two units of Quaternary sediments overlying bedrock. A major northwest-trending fault traverses the northeast portion of the target area, with vertical separation of the top of the basalt of at least 500 ft, down to the southeast. Northeast of this fault, bedrock consists of basalt flows of the Columbia River Basalt Group (Tbv); southwest of the fault, the basalt is overlain by several hundred feet of Pliocene-Pleistocene fluvial silt- and sandstone (QTaf). The Quaternary sediments consist of silt, sand, and gravel and were deposited by southward flowing catastrophic floodwater associated with drainage of Glacial Lake Missoula (Bretz and others, 1956; Waitt, 1985) and flowing south through the area. The floodwaters scoured an irregular surface on the bedrock units, then deposited an irregular body of pebble to boulder gravel (Qmc) on the scoured surface. The gravel is overlain by sand and silt deposited by waning floodwaters (Qmf). The Willamette and Mollala Rivers have cut into the flood deposits and have deposited small amounts of fluvial sediment on their floodplains. These sediments cannot be differentiated from the underlying flood sediments and are combined with the older material.

The geologic model consists of four bodies, one each of coarse and fine flood sediments (Qmc, Qmf) and one each of the bedrock units (Tbv, QTaf).

Shear-wave velocities are assigned as follows:

Qmf Two direct measurements, 160 and 266 m/sec, average 213 m/sec.

Qmc Two direct measurements 657 and 680 m/sec, average 668 m/sec.

QTaf No direct measurements. Sediments similar to QTaf at Newberg, McMinnville and Woodburn have a velocity ranging from 328 to 518 m/sec, with an average of 413 m/sec.

Tbv No direct measurements available. Average at St. Helens area is 957 m/sec.

Amplification hazard ranges from none in the northeast corner of the area (due to bedrock at or near the surface) to moderate in the north and southwest parts of the area (due to thick Qmf deposits). Amplification is low in much of the center of the area, where the Qmf deposits are thin or absent.

Liquefaction hazard ranges from nil in the northeast and central parts of the area (over Qmc gravel and bedrock) to moderate in the southwest and north parts of the area where there is thick Qmf.

Earthquake-induced landslide hazard is generally low, with the exception of areas of high to moderate hazard associated with bluffs along the rivers in the area and their major tributaries.

Relative hazard zones vary considerably, with large areas of Zone B in the southwest and north ends of the area, associated with Qmf deposits. Small areas of Zone A are the result of a combination of high landslide hazard along bluffs with amplification and liquefaction hazard. In the center of the area, there are large patches of Zones D and C, where the Qmf deposits are thin or absent.

LEBANON URBAN AREA

The Lebanon geologic model was developed using surface geologic data from Yeats and others (1991), Gannet and Caldwell, (1998), and O'Connor and others (in press); and subsurface data from 91 approximately located water wells. Landslides were mapped using air photo interpretation.

The geology consists of Quaternary river gravel (Qac) deposited on the floodplain of the Santiam River, and older river gravel, sand, and silt (QTac) deposited by the ancestral Santiam River over Tertiary volcanic and volcaniclastic bedrock (Tbv).

Shear-wave velocity is assigned to the units as follows:

Qac One direct measurement, 144 m / sec.

QTac One direct measurement, 244 m / sec.

Tbv Two direct measurements, 598 and 665 m / sec, average 631 m / sec.

Amplification hazard ranges from low to moderate, with moderate values associated with Qac and QTac gravel deposits on the valley floor, and low values associated with the Tbv bedrock in the surrounding hills.

Liquefaction hazard is nil, because the area is entirely gravel or bedrock.

Earthquake-induced landslide hazard ranges from low on the valley floors to mostly moderate in the surrounding hills. Some areas of high slope hazard in the hills are associated with existing landslides and the very steepest slopes.

Most of the valley floor is in relative hazard Zone C, and most of the surrounding hills are in Zone D. Some areas of the hills are in Zones C or D, associated with steep slopes or existing landslides.

SILVERTON-MOUNT ANGEL URBAN AREA

The Silverton-Mount Angel geologic model was developed using surface geologic data from Gannet and Caldwell (1998) and O'Connor and others (in press), air photo interpretation, and logs from 106 approximately located water wells.

The geology consists of bedrock of Miocene tuffaceous sedimentary rocks and lava flows of the Columbia River Basalt Group (Tbv) overlain by Miocene to Pleistocene alluvial silt and sandstone (QTaf), Pliocene to Quaternary fluvial gravel (QTac) and Pleistocene to Holocene silt and sand from glacial outburst floods (Bretz and others, 1956; Waitt, 1985) from Lake Missoula (Qmf). The northwest-trending Mount Angel fault runs through Mount Angel and was the likely source for the 1993 M 5.6 Scotts Mills earthquake. The Mount Angel fault offsets all the geologic units in the model except possibly Qmf, with a total southeast-side down displacement of at least 100m.

The geologic model consists of a body of QTaf, a body of QTac (including modern alluvial gravel), and a body of Qmf.

Shear-wave velocities are assigned as follows:

Qmf Two direct measurements, 184 and 196 m/sec, average 190 m/sec.

QTac One direct measurement, 438 m/sec.

QTaf One direct measurement, 818 m/sec.

Tbv Two direct measurements, 1,087 and 1,402 m/sec, average 1,244 m/sec.

Amplification hazard is nil in the southern part of the region, where bedrock is exposed at the surface in the Waldo Hills and at the bedrock hill (Mount Angel) just east of Mount Angel. Hazard is low to moderate in most of the valley floor areas, particularly where Qmf is thick.

Liquefaction hazard is nil in the bedrock areas described above and high over most of the valley floor, due to widespread deposits of Qmf.

Earthquake-induced landslide hazard is low throughout most of the valley floor, except for areas of moderate hazard along steeper slopes along minor streams. Hazard is moderate in the hills south of Silverton and at Mount Angel, with a few areas of high hazard associated with steep slopes along the valley of Silver Creek.

The southern half of the area is generally in relative hazard Zone D, with areas of Zones C and B associated with steep slopes. The northern half of the area is generally in Zone B, due to amplification and liquefaction hazards associated with Qmf. Some parts of the northern half are in Zone D, where Qmf is thin or absent.

STAYTON-SUBLIMITY-AUMSVILLE URBAN AREA

The Stayton-Sublimity-Aumsville geologic model was developed from geologic maps by Yeats and others (1991), Gannet and Caldwell (1998), and O'Connor and others (in press); and by subsurface data from 44 approximately located water wells.

The geology of the area consists of Quaternary and Pleistocene river gravel (Qac) filling a valley cut into Miocene volcanic and volcaniclastic bedrock units (Tbv). The geologic model consists of a body of Qac.

Shear-wave velocities were assigned as follows:

Qac One direct measurement 142 m/sec

Tbv Two direct measurements, 551 and 958 m/sec, average 754 m/sec.

Amplification hazard is moderate on the valley floor, due to thick Qac, and low in the surrounding hills.

Liquefaction hazard is nil throughout the area, because Qac is predominantly coarse gravel.

Earthquake-induced landslide hazard is low on the valley floor and generally moderate in the surrounding hills, except for a few areas of high hazard associated with the steepest slopes, particularly bluffs along the Santiam River.

Most of the area is in relative hazard Zone D, with areas of higher hazard associated with steep slopes.

Sweet Home Urban Area

The Sweet Home geologic model was developed using surface geologic data from Yeats and others (1991), Gannet and Caldwell (1998), and O'Connor and others (in press); and subsurface data from 49 approximately located water wells. Landslides were mapped using air photo interpretation.

The geology consists of Quaternary fluvial gravel and sand (Qac) filling the valley of the Santiam River. The Qac is deposited on Tertiary volcanic and volcaniclastic bedrock. (Tbv). The model consists of a body of Qac.

Shear-wave velocities are assigned as follows:

Qac One direct measurement, 203 m/sec.

Tbv One direct measurement, 855 m/sec.

Amplification hazard is low to moderate along the Santiam River valley floor, where there is significant thickness of Qac, and nil in the adjacent bedrock hills.

Liquefaction hazard is nil throughout the area, because the Qac is mostly coarse gravel.

Earthquake-induced landslide hazard is low on the valley floor and generally moderate on the adjacent hills. A few areas of high landslide hazard occur in the hills, where there are existing slides.

Most of the area is in relative hazard Zone D, with a band of Zone C along the Santiam River associated with thick Qac. Some patches of Zone B occur in the hills associated with steep slopes and existing landslides.

WOODBURN-HUBBARD URBAN AREA

The Woodburn-Hubbard geologic model was developed using surface geologic information from Gannet and Caldwell (1998), air photo interpretation, and interpretation of logs from 109 approximately located water wells.

The geology consists of two units of latest Pleistocene silt, deposited by catastrophic Missoula floods (Bretz and others, 1956; Waitt, 1985) on older Pleistocene fluvial, clay, sand, and gravel (QTaf). The upper unit of flood silt (Qmf1) is brown, the lower unit (Qmf2) is blue or gray. The underlying Pleistocene alluvium is composed of clay, sand and gravel. The geologic model consists of a body of Qmf1, a body of Qmf2 and a body of QTac.

Shear-wave velocities are assigned as follows:

Qmf1 Four direct measurements, 211 to 247 m/sec, average 233 m/sec.

Qmf2 Four direct measurements, 303 to 366 m/sec, average 343 m/sec.

QTaf Two direct measurements, 396 and 415 m/sec, average 405 m/sec.

Amplification hazard is moderate throughout the area.

Liquefaction hazard is low throughout the area.

Earthquake-induced landslide hazard is low throughout the area, except for small areas of moderate hazard associated with the walls of small stream valleys.

Most of the area is in relative hazard Zone C, with some areas of Zone B associated with steep slopes along minor stream valleys.

ACKNOWLEDGMENTS

Geological models were reviewed by Marshall Gannett and Jim O'Connor of the U.S. Geological Survey (USGS) Water Resources Division, Ken Lite of the Oregon Water Resources Department, Dr. Ray Wells of the USGS, Dr. Curt Peterson of Portland State University, Dr. Jad D'Allura of Southern Oregon University, and Dr. John Beaulieu, Gerald Black, and Dr. George Priest of the Oregon Department of Geology and Mineral Industries. The reports were reviewed by Gerald Black and Mei Mei Wang. Marshall Gannett and Jim O'Connor provided unpublished digital geologic data that were helpful in building the geologic models. Dr. Marvin Beeson provided unpublished geologic mapping. We are very grateful to all of these individuals for their generous assistance.

BIBLIOGRAPHY

Andrus, R.D., and Stokoe, K.H., 1997, Liquefaction resistance based on shear-wave velocity (9/18/97 version), in Youd, T.L., and Idriss, I.M., eds., Proceedings of the NCEER Workshop on Evaluation of Liquefaction Resistance of Soils, Jan. 4–5, Salt Lake City, Utah: Buffalo, N.Y., National Center for Earthquake Engineering Research Technical Report NCEER-97-0022, p. 89–128.

Atwater, B.F., 1987, Evidence for great Holocene earthquakes along the outer coast of Washington State: Science, v. 236, p. 942–944.

Atwater, B.F., and Hemphill-Haley, 1997, Recurrence intervals for great earthquakes of the past 3,500 years at northeastern Willapa Bay, Washington: U.S. Geological Survey Professional Paper 1576, 108 p.

Baldwin, E.M., 1964, Geology of the Dallas and Valsetz quadrangles, rev. ed.: Oregon Department of Geology and Mineral Industries Bulletin 35, 56 p., 1 map 1:62,500.

Beaulieu, J.D., 1977, Geologic hazards of parts of northern Hood River, Wasco, and Sherman Counties, Oregon: Oregon Department of Geology and Mineral Industries Bulletin 91, 95 p., 10 maps.

Beaulieu, J.D., and Hughes, P.W., 1975, Environmental geology of western Coos and Douglas Counties, Oregon: Oregon Department of Geology and Mineral Industries Bulletin 87, 148 p., 16 maps.

———1976, Land use geology of western Curry County, Oregon: Oregon Department of Geology and Mineral Industries Bulletin 90, 148 p., 12 maps.

Bela, J.L, 1981, Geology of the Rickreall, Salem West, Monmouth, and Sidney 7½' quadrangles, Marion, Polk, and Linn Counties, Oregon: Oregon Department of Geology and Mineral Industries Geological Map Series GMS–18, 2 pls., 1:24,000.

Bolt, B.A., 1993, Earthquakes: New York, W.H. Freeman and Co., 331 p.

Bretz, J.H., Smith, H.T.U., and Neff, G.E., 1956, Channeled Scabland of Washington: New data and interpretations: Geological Society of America Bulletin, v. 67, no. 8, p. 957–1049.

Brownfield, M.E., 1982, Geologic map of the Sheridan quadrangle, Polk and Yamhill Counties, Oregon: Oregon Department of Geology and Mineral Industries Geological Map Series GMS–23, 1:24,000.

Brownfield, M.E., and Schlicker, H.G., 1981, Preliminary geologic map of the McMinnville and Dayton quadrangles, Oregon: Oregon Department of Geology and Mineral Industries Open-File Report O–81–6, 1:24,000.

FEMA (Federal Emergency Management Agency), 1995, NEHRP recommended provisions for seismic regulations for new buildings, 1994 edition, Part 1: Provisions: Washington, D.C., Building Seismic Safety Council, FEMA Publication 222A / May 1995, 290 p.

Frankel, A., Mueller, C., Barnhard, T., Perkins, D., Leyendecker, E.V., Dickman, N., Hanson, S., and Hopper, M., 1996, National seismic hazard maps, June 1996 documentation: U.S. Geological Survey Open-File Report 96–532, 110 p.

Gannett, M.W., and Caldwell, R.R., 1998, Geologic framework of the Willamette Lowland aquifer system: U.S. Geological Survey Professional Paper 1424–A, 32 p., 8 pls.

Geomatrix Consultants, Inc., 1995, Seismic design mapping, State of Oregon: Final Report to Oregon Department of Transportation, Project no. 2442, var. pag.

Heaton, T.H., and Hartzell, S.H., 1987, Earthquake hazards on the Cascadia subduction zone: Science, v. 236, no. 4798, p. 162–168.

Hunter, J.A., Pullan, S.E., Burns, R.A., and Good, R.L., 1984, Shallow seismic reflection mapping of the overburden-bedrock interface with an engineering seismograph——Some simple techniques: Geophysics, v. 49, p. 1381–1385.

ICBO (International Conference of Building Officials), 1997, 1997 Uniform building code, v. 2, Structural engineering design provisions: Whittier, Calif., International Conference of Building Officials, 492 p.

Kanamori, H., 1977, The energy release in great earthquakes: Journal of Geophysical Research, v. 82, p. 2981–2987.

Mabey, M.A., Black, G.L., Madin, I.P., Meier, D.B., Youd, T.L., Jones, C.F., and Rice, J.B., 1997, Relative earthquake hazard map of the Portland metro region, Clackamas, Multnomah, and Washington Counties, Oregon: Oregon Department of Geology and Mineral Industries Interpretive Map Series IMS–1, 1:62,500.

Madin, I.P., and Mabey, M.A., 1996, Earthquake hazard maps for Oregon: Oregon Department of Geology and Mineral Industries Geological Map Series GMS–100.

Madin, I.P., Priest, G.R., Mabey, M.A., Malone, S., Yelin, T.S., and Meier, D., 1993, March 25, 1993, Scotts Mills earthquake—western Oregon's wake-up call: Oregon Geology, v. 55, no. 3, p. 51–57.

National Research Council, Commission on Engineering and Technical Systems, Committee on Earthquake Engineering, 1985, Liquefaction of soils during earthquakes: Washington, D.C., National Academy Press, 240 p.

O'Connor, J.E., Sarna-Wojcicki, A., Wozniak, K.C., Polette, D.J., and Fleck, R.J., in press, Origin, extent, and thickness of Quaternary geologic units in the Willamette Valley, Oregon: U.S. Geological Survey Professional Paper 1620.

Priest, G.R., 1995, Explanation of mapping methods and use of the tsunami hazard maps of the Oregon coast: Oregon Department of Geology and Mineral Industries Open-File Report O–95–67, 95 p.

Priest, G.R., and Baptista, A.M., 1995, Tsunami hazard maps of coastal quadrangles, Oregon: Oregon Department of Geology and Mineral Industries Open-File Report O–95–09 through O–95–66 (amended 1997 by O–97–31 and O–97–32), 56 quadrangle maps (as amended).

Ramp, L., and Peterson, N.V., 1979, Geology and mineral resources of Josephine County, Oregon: Oregon Department of Geology and Mineral Industries Bulletin 100, 45 p., 3 geologic maps.

Schlicker, H.G., Deacon, R.J., Beaulieu, J.D., and Olcott, G.W., 1972, Environmental geology of the coastal region of Tillamook and Clatsop Counties; Oregon Department of Geology and Mineral Industries Bulletin 74, 164 p., 18 pls.

Schlicker, H.G., Deacon, R.J., Newcomb, R.C., and Jackson, R.L., 1974, Environmental geology of coastal Lane County, Oregon: Oregon Department of Geology and Mineral Industries Bulletin 85, 116 p., 3 maps.

Seed, H.B., and Idriss, I.M., 1982, Ground motions and soil liquefaction during earthquakes: Earthquake Engineering Institute Monograph, 134 p.

Snavely, P.D., Jr., MacLeod, N.S., Wagner, H.C., and Rau, W.W., 1976, Geologic map of the Cape Foulweather and Euchre Mountain quadrangles, Lincoln County, Oregon: U.S. Geological Survey Miscellaneous Investigations Series Map I–868, 1:62,500.

Ticknor, R., 1993, Late Quaternary crustal deformation on the central Oregon coast as deduced from uplifted wave-cut platforms: Bellingham, Wash., Western Washington University master's thesis, 70 p.

Trimble, D.E., 1963, Geology of Portland, Oregon, and adjacent areas: U.S. Geological Survey Bulletin 1119, 119 p.

Waitt, R.B., 1985, Case for periodic, colossal jökulhlaups from Pleistocene glacial Lake Missoula: Geological Society of America Bulletin, v. 96, no. 10, p. 1271–1286.

Walker, G.W., and McLeod, N.S., 1991, Geologic map of Oregon: U.S. Geological Survey Special Geologic Map, 1:500,000.

Wang, Y., Keefer, D.K., and Wang, Z., 1998, Seismic hazard mapping in Eugene-Springfield, Oregon: Oregon Geology, v. 60, no. 2, p. 31–41.

Wang, Y., and Leonard, W.J., 1996, Relative earthquake hazard maps of the Salem East and Salem West quadrangles, Marion and Polk Counties, Oregon: Oregon Department of Geology and Mineral Industries Geological Map Series GMS–105, 1:24,000.

Wang, Y., and Priest, G.R., 1995, Relative earthquake hazard maps of the Siletz Bay area, coastal Lincoln County, Oregon: Oregon Department of Geology and Mineral Industries Geological Map Series GMS–93, 1:12,000 and 1:24,000.

Wang, Z., Wang, Y., and Keefer, D.K., 1999, Earthquake-induced rockfall and slide hazard along U.S. Highway 97 and Oregon Highway 140 near Klamath Falls, Oregon, in Elliott, W.M., and McDonough, P., eds., Optimizing post-earthquake lifeline system reliability. Proceedings of the 5th U.S. Conference on Lifeline Earthquake Engineering, Seattle, Wash., August 12–14, 1999: Reston, Va., American Society of Civil Engineers, Technical Council on Lifeline Earthquake Engineering Monograph 16, p. 61–70.

Weaver, C.S., and Shedlock, K.M., 1989, Potential subduction, probable intraplate, and known crustal earthquake source areas in the Cascadia subduction zone, in Hayes, W.W., ed., Third annual workshop on earthquake hazards in the Puget Sound / Portland area, proceedings of Conference XLVIII: U.S. Geological Survey Open-File Report 89–465, p. 11–26.

Wiley, T.J., Sherrod, D.R., Keefer, D.K., Qamar, A., Schuster, R.L., Dewey, J.W., Mabey, M.A., Black, G.L., and Wells, R.E., 1993, Klamath Falls earthquakes, September 20, 1993—including the strongest quake ever measured in Oregon: Oregon Geology, v. 55, no. 6, p. 127–134.

Wilkinson, W.D., Lowry, W.D., and Baldwin, E.M., 1946, Geology of the St. Helens quadrangle, Oregon: Oregon Department of Geology and Mineral Industries Bulletin 31, 39 p., 1 map, 1:62,500.

Yamaguchi, D.K., Atwater, B.F., Bunker, D.E., Benson, B.E., and Reid, M.S., 1997, Tree-ring dating the 1700 Cascadia earthquake: Nature, v. 389, p. 922.

Yeats, R.S., Graven, E.P., Werner, K.S., Goldfinger, C., and Popowski, T., 1991, Tectonics of the Willamette Valley, Oregon: U.S. Geological Survey Open-File Report 91–441–P, 47 p.

Yelin, T.S., Tarr, A.C., Michael, J.A., and Weaver, C.S., 1994, Washington and Oregon earthquake history and hazards: U.S. Geological Survey Open-File Report 94–226–B, 11 p.

APPENDIX

1. Geologic Units Used in Table A–1

Qaf Fine-grained Quaternary alluvium; river and stream deposits of sand, silt, and clay

Qac Coarse-grained Quaternary alluvium; river and stream deposits of sand and gravel

Qmf Fine-grained Quaternary Missoula flood deposits; sand and silt left by catastrophic glacial floods

Qmc Coarse-grained Quaternary Missoula flood deposits; sand and gravel left by catastrophic glacial floods

Qmf1 Fine-grained Quaternary Missoula flood deposits; upper, oxidized low-velocity layer

Qmf2 Fine-grained Quaternary Missoula flood deposits; lower, reduced high-velocity layer

Qe Quaternary estuarine sediments; silt, sand, and mud deposited in bays and tidewater reaches of major rivers

Qs Quaternary sands; beach and dune deposits along the coast

Qmt Quaternary marine terrace deposits; sand and silt deposited during previous interglacial periods

QPe Pleistocene estuarine sediments; older sand and mud deposited in bays and tidewater reaches of rivers

QTac Older coarse-grained alluvium; sand and gravel deposited by ancient rivers and streams

QTaf Older fine-grained alluvium; sand and silt deposited by ancient rivers and streams

Grus Decomposed granite

Tbs Sedimentary bedrock

Tbv Volcanic bedrock

KJg Granite bedrock

KJm Metamorphic bedrock

2. TABLE A-1, MEASURED SHEAR-WAVE VELOCITIES[1]

URBAN AREA	SITE #	LAT	LONG	T-1	V-1	U-1	T-2	V-2	U-2	T-3	V-3	U-3	T-4	V-4	U-4
							IMS–7								
Dallas	Dalla01	44.9287	-123.3222	3.4	165	Qmf	0.0	755	Tbs	—	—	—	—	—	—
Dallas	Dalla02	44.9218	-123.3001	2.7	174	Qmf	0.0	780	Tbs	—	—	—	—	—	—
Hood River	Hoodr01	45.7057	-121.5268	4.5	145	Qaf	0.0	1,352	Tbv	—	—	—	—	—	—
Hood River	Hoodr02	45.6893	-121.5190	1.0	139	?	6.0	271	QTac	38.0	377	QTac	0.0	995	Tbv
McMinnville-Dayton	McMin01	45.2052	-123.2321	5.8	180	Qmf1	0.0	1,371	Tbv	—	—	—	—	—	—
McMinnville-Dayton	McMin02	45.2112	-123.1383	7.0	201	Qmf1	0.0	277	Qmf2	—	—	—	—	—	—
McMinnville-Dayton	McMin03	45.2290	-123.0655	5.6	213	Qmf1	31.7	241	Qmf2	25.3	460	QTaf	0.0	914	Tbs
Monmouth-Independence	Monm01	44.8649	-123.2181	2.3	169	Qmf	15.0	325	QTac	29.1	550	QTaf	0.0	1,138	Tbv
Monmouth-Independence	Monm02	44.8425	-123.2027	7.0	159	Qmf	21.1	275	QTac	0.0	403	QTaf	—	—	—
Newberg-Dundee	Newb01	45.3123	-122.9494	4.9	220	Qmf1	0.0	513	Tbs	—	—	—	—	—	—
Newberg-Dundee	Newb02	45.2945	-122.9735	7.9	162	Qmf1	0.0	330	QTaf	—	—	—	—	—	—
St. Helens-Scappoose	STH01	45.8516	-122.8104	1.0	88	Qaf	0.0	1,204	Tbv	—	—	—	—	—	—
St. Helens-Scappoose	STH02	45.8562	-122.8364	1.0	40	?	0.0	830	Qac	—	—	—	—	—	—
St. Helens-Scappoose	STH03	45.8619	-122.7992	1.5	132	Qaf	0.0	710	Qac	—	—	—	—	—	—
Sandy	Sandy01	45.4029	-122.2745	4.5	286	Tbs	0.0	610	Tbs	—	—	—	—	—	—
Sheridan	Sher01	45.0948	-123.3898	3.4	125	Qmf	0.0	749	Tbs	—	—	—	—	—	—
Willamina	Willa01	45.0769	-123.4811	1.0	124	Qmf	3.0	386	QTaf?	0.0	773	Tbs	—	—	—
							IMS–8								
Canby-Aurora	Canb01	45.2682	-122.6859	2.5	266	Qmf	0.0	680	Qmc	—	—	—	—	—	—
Canby-Aurora	Canb02	45.2550	-122.6979	3.5	160	Qmf	0.0	657	Qmc	—	—	—	—	—	—
Lebanon	Lebanon01	44.5293	-122.9104	3.0	144	Qac	0.0	598	Tbv	—	—	—	—	—	—
Lebanon	Lebanon02	44.5517	-122.8945	4.9	244	QTac	0.0	665	Tbv	—	—	—	—	—	—
Silverton	Silvert01	45.0166	-122.7881	1.0	196	Qmf	3.0	818	QTaf	0.0	1,402	Tbv	—	—	—
Mt. Angel	Mtag01	45.0731	-122.7897	3.7	184	Qmf	10.0	438	QTac	0.0	1,087	Tbv	—	—	—
Stayton	Stayt01	44.8311	-122.7879	3.0	216	?	0.0	551	Tbv	—	—	—	—	—	—
Stayton	Stayt02	44.8047	-122.8014	1.8	142	Qac	0.0	958	Tbv	—	—	—	—	—	—
Sweet Home	Sweet01	44.3955	-122.7234	6.1	203	Qac	0.0	855	Tbv	—	—	—	—	—	—
Woodburn-Hubbard	Hub01	45.1871	-122.8026	1.0	101	?	11.2	244	Qmf1	0.0	364	Qmf2	—	—	—
Woodburn-Hubbard	Wood01	45.1451	-122.8228	6.1	247	Qmf1	33.5	341	Qmf2	0.0	396	QTaf	—	—	—
Woodburn-Hubbard	Wood02	45.1350	-122.8695	6.7	230	Qmf1	0.0	366	Qmf2	0.0	415	QTaf	—	—	—
Woodburn-Hubbard	Wood03	45.1538	-122.8499	4.5	211	Qmf1	0.0	303	Qmf2	—	—	—	—	—	—

[1] Measurements are for up to four successive identified layers (1 to 4) numbered from the surface down. T = thickness of layer (m); V = Shear-wave veolocity (m/s); U = Identified rock unit (see Appendix 1). Where thickness measurements did not reach bottom of layer, thickness is given as 0.0. Measurements with queried unit identifications were ignored.

2. TABLE A-1, MEASURED SHEAR-WAVE VELOCITIES, CONTINUED

URBAN AREA	SITE #	LAT	LONG	T-1	V-1	U-1	T-2	V-2	U-2	T-3	V-3	U-3	T-4	V-4	U-4
						IMS–9									
Ashland	Ashl01	42.2084	-122.7127	2.0	194	Qaf	6.2	720	Grus	0.0	1,220	Kjg	—	—	—
Ashland	Ashl02	42.1912	-122.6857	8.5	327	Qaf	13.5	640	Grus	0.0	1,015	Kjg	—	—	—
Cottage Grove	Cottage01	43.7856	-123.0651	3.4	219	Qac	0.0	973	Tbs	—	—	—	—	—	—
Cottage Grove	Cottage02	43.7968	-123.0331	3.6	187	Qac	0.0	1,270	Tbs	—	—	—	—	—	—
Grants Pass	Grantp01	42.4578	-123.3286	2.4	257	Qac	0.0	506	Grus?	—	—	—	—	—	—
Grants Pass	Grantp02	42.4458	-123.3135	1.5	134	Qaf	7.0	371	Qac	0.0	925	Grus	—	—	—
Grants Pass	Grantp03	42.4244	-123.3449	0.6	321	?	2.1	554	Qac	0.0	868	Grus	—	—	—
Roseburg	Roseb01	43.2159	-123.3668	6.0	181	Qac	0.0	944	Tbv	—	—	—	—	—	—
Sutherlin	Sutherl01	43.3822	-123.3306	5.0	426	Qaf	0.0	842	Tbs	—	—	—	—	—	—
Oakland	Oakland1	43.4221	-123.2988	9.1	198	Qaf	0.0	1,079	Tbs	—	—	—	—	—	—
						IMS–10									
Astoria	Ast01	46.1889	-123.8169	10.0	181	Qs	0.0	523	Tbs	—	—	—	—	—	—
Astoria	Ast02	46.1553	-123.8254	5.0	70	Qe	0.0	133	Qs	—	—	—	—	—	—
Astoria	Ast03	46.1530	-123.8877	8.2	81	Qe	0.0	151	Qs	—	—	—	—	—	—
Warrenton	War02	46.2049	-123.9516	0.0	190	Qs	—	—	—	—	—	—	—	—	—
Warrenton	War01	46.1724	-123.9209	5.5	95	Qe	0.0	210	Qs	—	—	—	—	—	—
Brookings	Brook01	42.0570	-124.2809	0.0	183	?	6.0	481	Qmt	0.0	1,172	Kjm	—	—	—
Coquille	Coquil01	43.1854	-124.1941	9.5	191	Qaf	0.0	385	Tbs	—	—	—	—	—	—
Coquille	Coquil02	43.1759	-124.1981	27.0	151	Qaf	0.0	589	Tbs	—	—	—	—	—	—
Florence-Dunes City	Floren01	43.9920	-124.1062	11.2	218	Qs	0.0	313	Qs	—	—	—	—	—	—
Florence-Dunes City	Floren02	43.9714	-124.1008	4.4	241	Qs	0.0	371	Qs	—	—	—	—	—	—
Florence-Dunes City	DuneC01	43.9266	-124.0989	4.0	174	Qs	0.0	576	Tbs	—	—	—	—	—	—
Lincoln City	Lincoln01	44.9805	-124.0020	4.3	185	Qmt	0.0	958	Tbs	—	—	—	—	—	—
Lincoln City	Lincoln02	44.9305	-124.0121	0.0	282	Qs	—	—	—	—	—	—	—	—	—
Lincoln City	Lnd01	44.9378	-124.0172	12.0	334	Qmt	5.0	626	Tbs	—	—	—	—	—	—
Lincoln City	Lnp01	44.9142	-124.0179	8.0	225	Qs	—	—	—	—	—	—	—	—	—
Lincoln City	Lnp02	44.9297	-124.0108	5.0	129	Qs	9.0	193	Qs	—	—	—	—	—	—
Lincoln City	Lnp05	44.9191	-124.0252	9.0	242	Qs	—	—	—	—	—	—	—	—	—
Newport	Newp01	44.6399	-124.0504	1.0	200	Qs?	6.7	448	Qmt	0.0	613	Tbs	—	—	—
Newport	Newp02	44.6156	-124.0608	17.0	324	Qs	0.0	419	Qs	—	—	—	—	—	—
Reedsport-Winchester Bay	Reedp01	43.7179	-124.0914	6.4	89	Qe	8.5	144	QPe	0.0	262	QPe?	—	—	—
Reedsport-Winchester Bay	Reedp02	43.6919	-124.1220	3.9	142	QPe	0.0	749	Tbs	—	—	—	—	—	—
Seaside-Cannon Beach	Seas01	45.9786	-123.9289	6.7	274	Qs	0.0	365	Qs	—	—	—	—	—	—
Seaside-Cannon Beach	Seas02	46.0093	-123.9144	12.2	170	Qs	0.0	262	Qs	—	—	—	—	—	—
Seaside-Cannon Beach	Seas03	46.0302	-123.9196	15.5	208	Qs	0.0	280	Qs	—	—	—	—	—	—
Tillamook	Tillam01	45.4629	-123.7993	2.4	335	QTac	0.0	610	Tbs	—	—	—	—	—	—
Tillamook	Tillam02	45.4356	-123.8423	17.0	82	Qe	0.0	308	QTac	—	—	—	—	—	—
Tillamook	Tillam03	45.4712	-123.8503	17.4	83	Qe	0.0	250	QTac	—	—	—	—	—	—

3. Collection and Use of Shear-Wave Velocity Data

This section describes our technique for collecting and applying the shear-wave velocity data shown in the preceding table (Table A-1). The table is also available on the accompanying CD-ROM disk as a Microsoft ExcelTM spreadsheet.

SH-wave data were collected by means of a 12-channel Bison 5000 seismograph with 8-bit instantaneous floating point and 2048 samples per channel. The data were recorded at a sampling rate between 0.025 and 0.5 ms, depending upon site conditions. The energy source for SH-wave generation is a 1.5 m section of steel I-beam struck horizontally by a 4.5-kg sledgehammer. The geophones used for recording SH-wave data were 30-Hz horizontal component Mark Product geophones. Spacing between the geophones is 3.05 m (10 ft). We used the walkaway method (Hunter and others, 1984), in which a group of 12 in-line geophones remained fixed and the energy source was "stepped out" through a set of predefined offsets. Depending upon site-geological conditions, the offsets of 3.05 m (10 ft), 30.5 m (100 ft), 61.0 m (200 ft), 91.5 m (300 ft), 122 m (400 ft), and 152.4 m (500 ft) were used. In order to enhance the SH-wave and reduce other phases, 5-20 hammer strikes on each site of the steel I-beam were stacked and recorded for each offset.

The SH-wave data were processed on a PC computer using the commercial software SIP by Rimrock Geophysics, Inc. (version 4.1, 1995). The key step for data processing is to identify the refractions from different horizons. Figure A-1 shows the composited SH-wave refraction profile generated from the individual offset records, at site McMin03 (Table A-1) near Dayton, Oregon. Four refractions, R1, R2, R3, and R4 are identified in the profile.

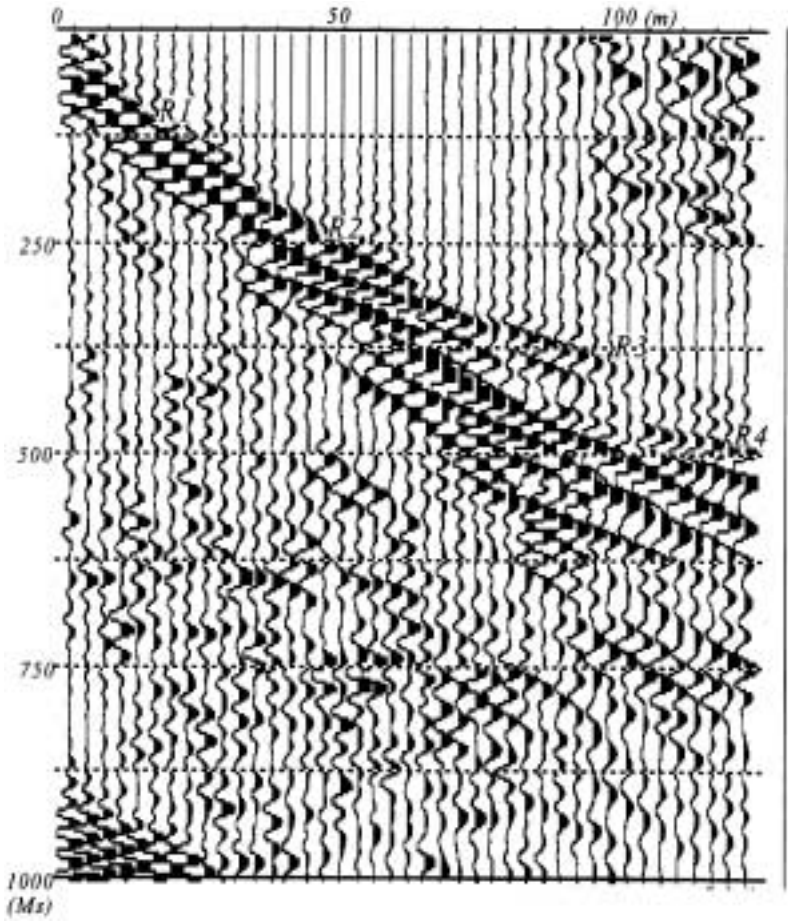

Figure A-1. Composited SH-wave refraction profile at site McMin03.

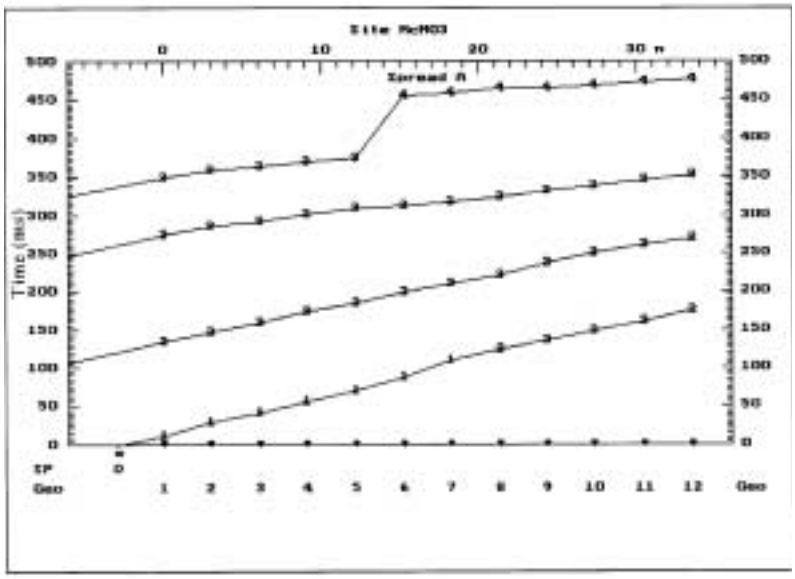

Figure A-2. Arrival time curves of the refractions at site McMin03.

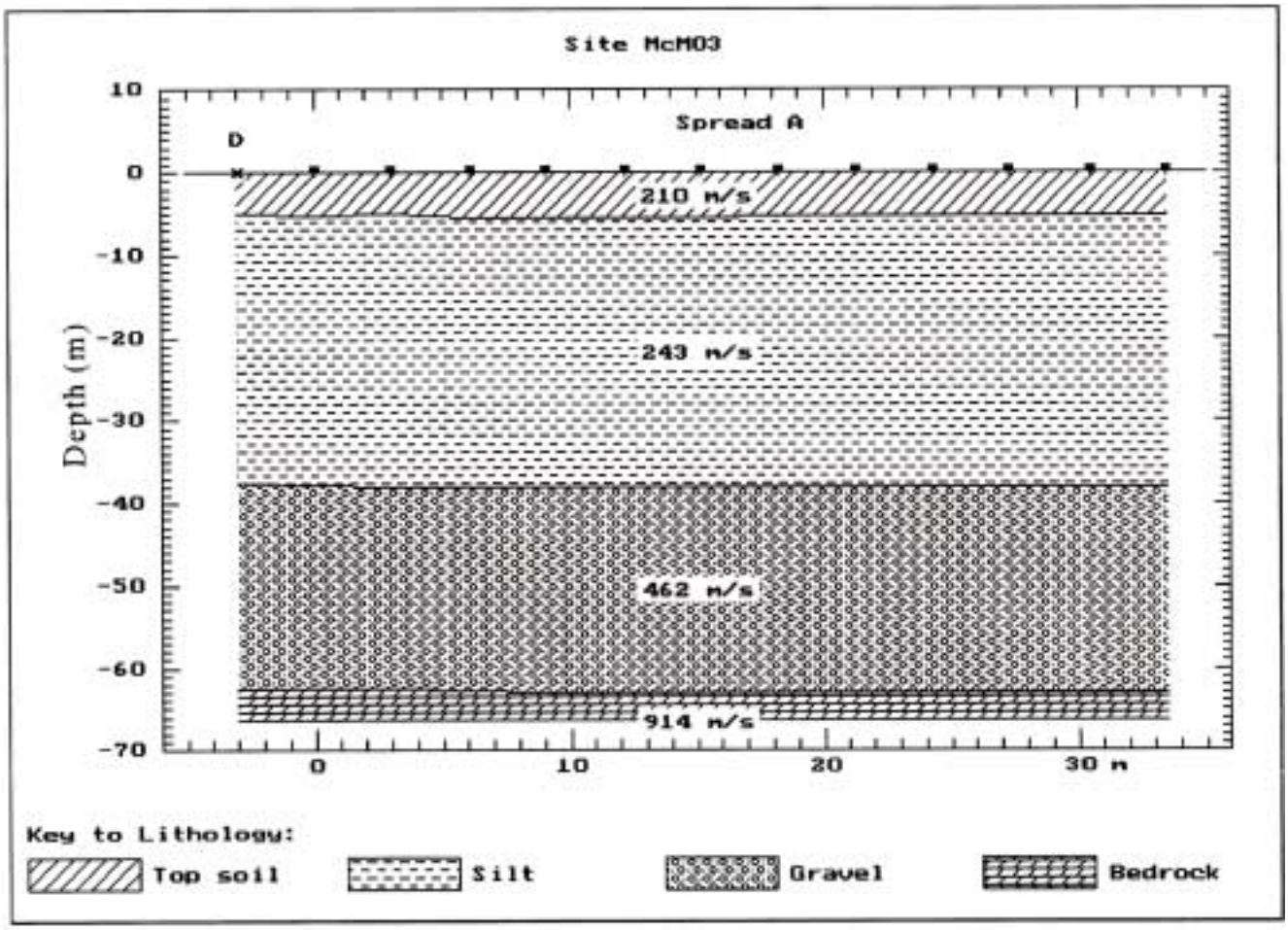

Figure A-3. Shear-wave velocity model interpreted from refraction data at site McMin03.

Arrival times of the refractions were picked interactively on the PC using the BSIPIK module in SIP. The arrival time data picked from each offset record were edited and combined in the SIPIN module to generate a data file for velocity-model deduction.

Figure A-2 shows the arrival times for the refractions identified in the profile (Figure A-1). The shear-wave velocity model is generated automatically using the SIPT2 module. Figure A-3 shows the shear-wave velocity model derived from the refraction data at site McMin03 (Figure A-1). The model is used to calculate an average shear-wave velocity.

The average shear-wave velocity (ns) over the upper 30 m of the soil profile is calculated with the formula of the Uniform Building Code (International Conference of Building Officials, 1997):

$$\boldsymbol{V}_s = 30\text{m} / \boldsymbol{\Sigma}\{d_i / \boldsymbol{V}_{si}\}$$

Where: d_i = thickness of layer i in meters and V_{si} = shear-wave velocity of layer i in m/s.

Based on the average shear-wave velocity and the UBC-97 soil profile categories as shown in Table 1 above (page 4), the UBC-97 soil classification map is generated with MapInfo® and Vertical Mapper®. Soil types SE and SF can not be differentiated from the average shear-wave velocity. SE and SF are differentiated based on geologic and geotechnical data, and engineering judgement.